NASA TM-87601

NASA Technical Memorandum 87601

NASA-TM-87601 19860001446

INVESTIGATION OF COMPOSITE MATERIAL PROPERTY REQUIREMENTS FOR SONIC FATIGUE RESEARCH

HOWARD V. L. PATRICK

AUGUST 1985

NASA
National Aeronautics and
Space Administration

Langley Research Center
Hampton, Virginia 23665

SUMMARY

This paper presents experimental techniques for determining the extensional and bending stiffness characteristics for symmetric laminates. Vibrational test techniques for determining the dynamic modulus and material damping are also discussed.

Partial extensional stiffness results initially indicate that the laminate theory used for predicting stiffness is accurate. It is clearly shown that the laminate theory can only be as accurate as the physical characterisitcs describing the lamina, which may vary significantly.

It is recommended that all of the stiffness characteristics in both extension and bending be experimentally determined to fully verify the laminate theory. Dynamic modulus should be experimentally evaluated to determine if static data adequately predicts dynamic behavior. Material damping should also be ascertained because laminate damping is an order of magnitude greater than found in common metals and can signficantly effect the displacement response of composite panels.

INTRODUCTION

Graphite-epoxy composite materials have become of great interest to the aeronautics and space industry because of their high strength and stiffness to weight ratios. Acoustically induced material fatigue is of concern because of the intense fluctuating pressure fields generated by aircraft and spacecraft propulsion systems on structures.

Scientists would like to mathematically predict the displacement response of composite panels to acoustically induced random pressure fields. The panel strains can be evaluated once the displacement response has been ascertained.

Various investigators (1-3)* have developed theories which predict the deflection response of symmetric laminate plates. Solution of these equations requires determination of the extensional and bending stiffness matrices which can be predicted theoretically (4) based upon certain physical characteristics of the lamina. This laminate theory is based upon the static experimental material characteristics of a single unidirectional lamina.

Concern exists about the validity of using static material properties in a dynamic analytic model. The modulus (a measure of stiffness) can be determined indirectly by mechanically vibrating laminate cantilever beams (5-8).

The investigation reported herein presents methods for experimentally verifying the static stiffness matrices for symmetric laminates. A technique for determining some important dynamic characteristics will also be addressed. Partial experimental data for the extensional matrix for a T300/5208 graphite-epoxy angle-ply laminate is also presented. This laminate plate consisted of nominally 1-mm (0.040-in.) thick 8-ply material having a lay-up of $[0°, 45°, -45°, 90°]_s$, where the subscript s denotes symmetric lay-up.

This study considered those factors that effect the behavior of composite materials. It was determined that dynamic behavior is of upmost importance and includes stiffness, material damping and structural damping characteristics. Verification of the laminate theory under dynamic as well as static conditions, thin versus thick plate and small versus large deflection conditions is required. Major factors controlling material characteristics include manufacturing and material variability as well as environmental conditions, especially moisture and temperature.

---

* refers to reference

Long term goals should include the study of fatigue characteristics with sinusoidal and random excitation with appropriate frequency distribution. Another important material characteristic is creep, the slow change of physical dimensions associated with prolonged exposure to stress and temperature. Finally, new composite construction (lay-up) and material compositions should also be investigated.

LIST OF SYMBOLS

a_o	base displacement amplitude
$\ddot{a}_o$	base acceleration amplitude
A_{ij}	extensional stiffness matrix
A'_{ij}	A^{-1}_{ij}, inverse stiffness matrix
B_{ij}	coupling stiffness matrix
B'_{ij}	B^{-1}_{ij}, inverse stiffness matrix
D_{ij}	bending stiffness matrix
D'_{ij}	D^{-1}_{ij}, inverse stiffness matrix
D_s	energy dissipated per cycle
E	static modulus of elasticity
E*	effective complex modulus
E'	dynamic modulus (storage modulus)
E''	loss modulus
G	shear modulus
h	beam thickness
I	area moment of inertia of beam cross section
k	lamina layer number
L	beam length

M	moment
N	force
$\bar{Q}_{ij}$	transformed reduced lamina stiffness
r	mode number
U_s	strain energy in beam at maximum displacement
V	shear force
w	beam deflection
x	distance along beam from fixed end
x_o	distance along beam from fixed end to center of strain gage
z_k	distance from laminate midplane to kth lamina layer
γ	beam shear strain
ε	beam extensional strain
η_s	specimen loss factor
κ	curvature
λ_r	eigenvalue of rth mode
μ	mass per unit length of beam
ν	damping ratio
ν_{12}	Poisson's ratio
σ	normal stress
τ	shear stress
ϕ_r	characteristic function describing beam-deflection curve
ω_r	angular resonance frequency of rth mode

BACKGROUND

Static Conditions

Classical laminate theory allows prediction of laminate stiffness characteristics based upon the physical characteristics of unidirectional lamina where:

$$A_{ij} = \sum_{k=1}^{N} (\bar{Q}_{ij})_k (z_k - z_{k-1})$$

$$B_{ij} = 1/2 \sum_{k=1}^{N} (\bar{Q}_{ij})_k (z_k^2 - z_{k-1}^2) \qquad [1]$$

$$D_{ij} = 1/3 \sum_{k=1}^{N} (\bar{Q}_{ij})_k (z_k^3 - z_{k-1}^3)$$

A_{ij} is called the extensional stiffness, B_{ij} the coupling stiffness, and D_{ij} the bending stiffness. Knowing the transformed reduced lamina stiffness $\bar{Q}_{ij}$ (4) and z_k, which is the distance from the plate middle surface to the k-th layer, the stiffness matrices can be calculated. The unidirectional reinforced plies (lamina) from which the laminates are constructed possess four engineering elastic constants E_{11}, the modulus in the direction of the reinforcing filamant, E_{22}, the modulus transverse to the filamant direction, G_{12}, the longitudinal shear modulus and, ν_{12}, Poisson's ratio. When a laminate is fabricated with materially orthotropic lamina, the stiffness reduces to a 3 by 3 symmetric matrix.

The assumption used in the derivation of the laminate theory are similar to those used in the standard hypothesis for plates and shells. This approach could actually be called the classical thin lamination or plate theory.

The basic stress and deformation hypothesis is based upon the assumption that the laminate consists of perfectly bonded laminae, bonds are assumed to infinitesimally thin as well as non-shear-deformable. That is, the displacement are continuous across lamina boundaries so that no lamina can slip relative to one another. The laminate acts, therefore, as a single layer with very special properties, but nevertheless acts as a single layer of material (4).

If the laminate is thin, a line originally straight and perpendicular to the middle surface of the laminate is assumed to remain straight and perpendicular to the middle surface when the laminate is extended and bent. This assumption is equivalent to ignoring shear strains perpendicular to the middle surface, i.e., $\gamma_{xz} = \gamma_{yz} = 0$. In addition, the normals are presumed to have constant length so that the strain perpendicular to the middle surface is ignored, i.e., $\varepsilon_z = 0$ (4).

Figure 1 shows a typical stress and strain variations of a laminate of dissimilar lamina. As previously stated, the strain is assumed to vary linearly across the plate but $\bar{Q}_{ij}$ can be different for each lamina layer. Because of this difference in lamina stiffness, the stress variation through the laminate thickness is not necessarily linear as shown in Figure 1.

The force-moment relationships for a laminate, where ε_x^o, ε_y^o, and γ_{xy}^o are the normal and shear strains at the middle surface κ_x, κ_y, and κ_{xy} the curvature, is:

$$\begin{Bmatrix} N_x \\ N_y \\ N_{xy} \end{Bmatrix} = \begin{bmatrix} A_{11} & A_{12} & A_{16} \\ A_{12} & A_{22} & A_{26} \\ A_{16} & A_{26} & A_{66} \end{bmatrix} \begin{Bmatrix} \varepsilon_x^o \\ \varepsilon_y^o \\ \gamma_{xy}^o \end{Bmatrix} + \begin{bmatrix} B_{11} & B_{12} & B_{16} \\ B_{12} & B_{22} & B_{26} \\ B_{16} & B_{26} & B_{66} \end{bmatrix} \begin{Bmatrix} \kappa_x \\ \kappa_y \\ \kappa_{xy} \end{Bmatrix}$$

$$\begin{Bmatrix} M_x \\ M_y \\ M_{xy} \end{Bmatrix} = \begin{bmatrix} B_{11} & B_{12} & B_{16} \\ B_{12} & B_{22} & B_{26} \\ B_{16} & B_{26} & B_{66} \end{bmatrix} \begin{Bmatrix} \varepsilon_x^o \\ \varepsilon_y^o \\ \gamma_{xy}^o \end{Bmatrix} + \begin{bmatrix} D_{11} & D_{12} & D_{16} \\ D_{12} & D_{22} & D_{26} \\ D_{16} & D_{26} & D_{66} \end{bmatrix} \begin{Bmatrix} \kappa_x \\ \kappa_y \\ \kappa_{xy} \end{Bmatrix} \qquad [2]$$

where N_x, N_y, and N_{xy} are the normal and shear forces per unit width, M_x and M_y are the bending moments per unit width in the x and y directions respectfully, and M_{xy} is the twisting moment per unit width.

For the symmetric case we are considering, the laminas are geometrically symmetric around the middle surface as well as materially similar, the coupling matrix B_{ij} vanishes. Further simplifications can exist if the laminate is extensionally balanced, $A_{12} = A_{26} = 0$, i.e. no shear coupling, or balanced in bending where $D_{16} = D_{26} = 0$, i.e. no coupling between bending and twisting.

When performing experiments, the loads are applied and the resulting deformations are measured. The resultant forces and moments are written in terms of the middle surface extensional strains and curvatures as:

$$\left\{\begin{array}{c} N \\ \hline M \end{array}\right\} = \left[\begin{array}{c|c} A & B \\ \hline B & D \end{array}\right] \left\{\begin{array}{c} \varepsilon^o \\ \hline \kappa \end{array}\right\} \qquad [3]$$

Because of experimental techniques, the deformations are the dependent variables and it is advantageous to invert the force-moment equation. For a symmetric laminate, the coupling matrix B vanishes, and the inversion is simply (10):

$$\left\{\begin{array}{c} \varepsilon^o \\ \hline \kappa \end{array}\right\} = \left[\begin{array}{c|c} A^{-1} & 0 \\ \hline 0 & D^{-1} \end{array}\right] \left\{\begin{array}{c} N \\ \hline M \end{array}\right\} \qquad [4]$$

Note that this relationship is much more complex if the laminate is not symmetric. Let us denote $A^{-1} = A'$ and $D^{-1} = D'$ and in expanding we have:

$$\begin{Bmatrix} \varepsilon_x^o \\ \varepsilon_y^o \\ t_{xy}^o \end{Bmatrix} = \begin{bmatrix} A'_{11} & A'_{12} & A'_{16} \\ A'_{12} & A'_{22} & A'_{26} \\ A'_{16} & A'_{26} & A'_{66} \end{bmatrix} \begin{Bmatrix} N_x \\ N_y \\ N_{xy} \end{Bmatrix} \quad [5]$$

$$\begin{Bmatrix} \kappa_x \\ \kappa_y \\ \kappa_{xy} \end{Bmatrix} = \begin{bmatrix} D'_{11} & D'_{12} & D'_{16} \\ D'_{12} & D'_{22} & D'_{26} \\ D'_{16} & D'_{26} & D'_{66} \end{bmatrix} \begin{Bmatrix} M_x \\ M_y \\ M_{xy} \end{Bmatrix} \quad [6]$$

Verification of one set of stiffnesses implies verification of the other set because the two sets, A and D, and A' and D', are the inverse of one another. The stiffness matrices can readily be calculated from the inverted form.

Dynamic Conditions

Because lamina material characteristics obtained from static tests are used to predict the laminate stiffness characteristics, the dynamic stiffness characteristics should also be addressed. Schultz and Tsai report (6) up to 20% variation of stiffness between dynamic and static measurements for 6 and 8-layer angle-ply glass/epoxy laminates. Other investigators (7) using two-layer cross-ply E-glass/epoxy laminates, have found very good agreement between static and dynamic stiffness.

Both of these investigations are based upon mechanically vibrating cantilever beams at resonance and then calculating the dynamic modulus E', based upon classical vibration analysis. This modulus is a measure of stiffness and when compared to values obtained from static tests, gives an indication if the stiffness is different under dynamic conditions.

STATIC EXPERIMENTAL TECHNIQUES

Extensional Stiffness in Tension

The extensional matrix coefficients can readily be determined by applying unaxial forces to the laminate in preferred directions. Let us first consider the case where, $N_y = N_{xy} = 0$, then from Equation 5 we have, $\varepsilon_x^o = A'_{11} N_x$, $\varepsilon_y^o = A'_{12} N_x$ and $t_{xy}^o = A'_{16} N_x$. Because the laminates we are considering are symmetric, there is no coupling between extension and bending, i.e. $B_{ij} = 0$, and the strains remain the same across the surface, $\varepsilon^o = \varepsilon$, therefore $A'_{11} = \varepsilon_x/N_x$, $A'_{12} = \varepsilon_y/N_x$ and $A'_{16} = \gamma_{xy}/N_x$. We need only apply a known uniaxial stress to a specimen, measure the surface strain and determine the coefficients.

Similarly, we can apply a uniaxial force N_y where $N_x = N_{xy} = 0$ and measure the surface strain and determine $A'_{12} = \varepsilon_x/N_y$, $A'_{22} = \varepsilon_y/N_y$ and $A'_{26} = \gamma_{xy}/N_y$.

This extensional data can be determined by a simple tensile test using standard laboratory techniques (11). Figure 2 shows the specimen size recommended for composites. A simple tensile testing machine is used for applying loads and instrumentation for a strain gage rosette is required, in addition, two specimens are needed to obtain adequate information. These specimens, as shown in Figure 3, consist of; first sample with its outer fibers aligned with the longitudinal axis (x-direction); and the second with its outer fiber 90° to the longitudinal axes. A 45° strain gage rosette should be placed on one of the surfaces near the middle of the test specimen. The shear strain can be obtained from the relationship

$$\gamma_{xy} = 2\,\varepsilon_{OB} - (\varepsilon_x + \varepsilon_y)$$

with the rosette layout shown in Figure 4. From these two test specimens we then can determine A'_{11}, A'_{22}, A'_{12}, A'_{16}, and A'_{26} as described above.

A minimum of three specimens each, of the 0°, and 90° orientations, should be tested. More reliable data could also be obtained by having strain gage rosettes on both surfaces and base the strain values on the average of the two gages. This procedure should result in statistically significant data.

Extensional Stiffness in Shear

The stiffness coefficient A'_{66} is obtained by placing a laminate specimen in pure shear. For this case $N_x = N_y = 0$ and from Equation 5 we have $A'_{66} = \gamma_{xy}/N_{xy}$. We can also verify the shear coupling coefficients where $A'_{16} = \varepsilon_x/N_{xy}$ and $A'_{26} = \varepsilon_y/N_{xy}$; both of which can also be determined during the tension tests.

There exists no standard shear tests for composite laminates. Spiegel (12) and Herakovich (13) discuss the advantages and disadvantages of various types of shear tests. The technique that is probably the most valid is the picture-frame shear test (14). Validity is based upon the specimen being in pure shear and void of extraneous normal forces or moments associated with the technique, stress concentrations or fixture characteristics. The major disadvantage of the picture-frame shear test is the large size of the test specimen which is typically on the order of 44.5-cm (17.5-in.) square (14).

A shear test technique that is considered reasonably accurate and also uses a small test specimen is the double V-notch shear test which is commonly called the Iosipescu Shear Test (15). A slight variation of this test technique is called the asymmetrical Four-Point Bend (AFPB) test (16). It has

been shown theoretically (12, 16) and experimentally (12) that the Iosipescu Shear Test is accurate when used with composite laminates, The AFPB Shear Test is probably the most accurate of the two methods. The Isoipescu Shear Test is comprised of a simple compression test fixture shown schematically in Figure 5.

Inspection of Figure 6 shows that at the double V-notch, the beam is in pure shear with no moment. The magnitude of the shear stress in the constant shear stress region is governed by external equilibruim requirements of the specimen and is seen to be just the applied load P. Iosipescu (15) showed that, because of the 90° V-notch in the test specimen, constant shear exists all of the way across the beam between the notches. To experimentally determine the shear stress we measure the normal strain at a 45° angle at the middle of the test specimen between the V-notches as related by the sketch of Mohr's circle in Figure 7. A small strain gage should be used because of the relatively small region of pure shear. Because the specimen is so narrow, the strain should be measured on both sides of the test specimen and the average value used on the applicable strain γ_{xy}. From Equation 5, we have $A'_{66} = \gamma_{xy}/N_{xy}$.

We could verify the shear coupling coefficients by measuring the strain using a strain gage rosette in the test region. Again from Equation 5, we would have $A'_{16} = \varepsilon_x/N_{xy}$ and $A'_{26} = \varepsilon_y/N_{xy}$. This particular measurement would probably be inaccurate because of the small size of the test section between the notches.

Bending Stiffness for Bending Moments

Examination of Equation 6 shows that we can determine the bending stiffness coefficients by applying pure bending moments to the test specimen.

For example, let $M_y = M_{xy} = 0$, we could then determine $D'_{11} = \kappa_x/M_x$, $D'_{12} = \kappa_y/M_x$, and $D'_{16} = \kappa_{xy}/M_x$. Similarly, we could take the case for $M_x = M_{xy} = 0$ and we would have $D'_{12} = \kappa_x/M_y$, $D'_{22} = \kappa_y/M_y$, and $D'_{26} = \kappa_{xy}/M_y$.

Let us examine what we mean by curvature, κ. Shown in Figure 8 is a plate in the xy plane where w_o is the midplane deflection in the z-direction and $\beta = \frac{\partial w_o}{\partial x}$. It can be readily shown (4) that the curvatures are; $\kappa_x = \frac{\partial^2 w_o}{\partial y^2}$, and $\kappa_{xy} = -2\frac{\partial^2 w_o}{\partial x \partial y}$. This curvature can be measured directly, or the deflection can be measured and then the curvature can be determined from the above relationships.

Optical holographic techniques can be used for determining the components of curvature by measuring the interference fringes (17-19). These measurements are valid for plates in anticlastic bending which is only applicable for laminates that do not have coupling between the pure bending moments, M_x and M_y, and the twisting moment M_{xy}, i.e., $D'_{16} = D'_{26} = 0$. In other words, holographic techniques can only be used if the bending matrix, D_{ij}, is balanced such as in cross-ply laminates. Major disadvantages of using holographic interferometry include the large instrumentation costs, difficulty and cost of measuring, interpreting the interference fringe patterns, and the difficulty of putting thin laminates 1-3 mm (0.04-0.12 in.) in appropriate bending under known conditions.

Various investigators (5-8) have used a technique for determining bending stiffness characteristics by using a simply loaded cantilever beam and measuring the strain near the support. A rectangular shaped beam has a

parabolic shear stress distribution in the x-z plane with a maximum value at the midplane but zero at the surfaces. We can, therefore, measure the strain at the surface due to the effects of curvature without being concerned with shear forces in the x-z plane,

$$\varepsilon_i^o + \frac{h}{2}\kappa_i = \varepsilon_i^u, \quad \text{where } i = x, y, xy, \quad \text{and } u = \text{upper surface}$$

or $$\varepsilon_i^o - \frac{h}{2}\kappa_i = \varepsilon_i^\ell, \quad \text{where } \ell = \text{lower surface.}$$

Because we have no normal stress at the midplane during bending, ε^o vanishes and we have

$$\frac{h}{2}\kappa_i = \varepsilon_i^u \quad \text{and} \quad -\frac{h}{2}\kappa_i = \varepsilon_i^\ell. \qquad [7]$$

Experiments should be performed using two sets of cantilever beams, one with the beam axis with the outer fibers aligned with the beam axis and the other with the outer fiber aligned 90° (perpendicular) with the beam axis or shown in Figure 9. Strain gages should be mounted on both surfaces of the cantilever beam near the support where the magnitude of the moment is large. From these strain gages, we can determine ε_x, ε_y, and γ_{xy}; with the upper side in tension and the lower one in compression. Note that the magnitude of the moment at the center of each strain gage is different because of slightly different geometrically locations relative to the end of the beam, as can be seen from Figure 4.

Because of the small loads required to bend the beam in the range of curvature desired, much care must be used in the experimental procedure, as well as the size of the beam. A reasonable beam size would be in the order of 1 in. wide by 6-in. long. The concentrated load should actually be a distributed load along a transverse line at the end of the beam as shown in Figure 10.

Let us examine the case for the simply loaded cantilever beam with $M_y = M_{xy} = 0$; from Equation 7: $\frac{h}{2}\kappa_x = \varepsilon_x$ and from Equation 6: $\kappa_x = D'_{11}M_x$ therefore, $D'_{11} = \frac{2\varepsilon_x}{hM_x}$; similarly we have $D'_{12} = \frac{2\varepsilon_y}{hM_x}$ and $D'_{16} = \frac{2\gamma_{xy}}{hM_x}$.

For the beam with the orthogonal outer fiber direction where, $M_x = M_{xy} = 0$, we would have from Equations 6 and 7, $D'_{12} = \frac{2\varepsilon_x}{hM_y}$, $D'_{22} = \frac{2\varepsilon_y}{hM_y}$, and $D'_{26} = \frac{2\gamma_{xy}}{hM_y}$. Care should be taken with the sign of the coefficient because of the direction of the curvature; basing the strain magnitude upon the average of the upper end lower surface strain gages, while taking into consideration, one is in tension and the other in compression.

Bending Stiffness for Twisting Moments

The last bending stiffness coefficient is associated with the twisting moment M_{xy}. The saddle test or four point loading of a plate can be used to determine D_{66} as well as the shear modulus, G. This technique has been successfully used for laminate plates (6, 20). The saddle test is accomplished by placing four equal forces at the corners of a square plate as shown in Figure 11. The forces are perpendicular to the plate with those forces at the first and third (diagonal) corners being upward and the other two forces downward. The corner loads create a twisting moment resulting in the square plate assuming a hyperbolic paraboloid, or a saddle shape. The matrix coefficent, D_{66}, is calculated using the relationship (4, page 181)

$$D_{66} = \frac{PL^2}{4w_c}$$

where the P is the applied load at the corners, L is the diagonal (corner-to-corner) distance of the plate and w_c the deflection at the corners with respect to the center of the plate. The shear modulus can also be calculated using the relationships (20)

$$G = \frac{3PL^2}{2w_c h^3}$$

where h is plate thickness.

Extreme care must be used in performing the saddle test because of the very small forces, less than one Newton, required when testing 1-2 mm (0.04-0.08 in.) thick plates. Alignment becomes critical and instrumentation used for measuring the corner deflection, w_c should not impose forces on the plate.

ENVIRONMENTAL CONSIDERATIONS

The effects of environmental conditions on static and dynamic properties is of utmost importance. High temperature and diffusion of moisture into resin materials are of major concern. It has been reported (21) that a hot moist environment alters the stiffness and damping characteristics of graphite epoxy composites. Some investigators (22) performing static flexural tests of graphite/epoxy beams, concluded that moisture and temperature can actually change the mode of failure.

Another parameter that affects material characteristics of composite materials is the time parameter. Resin/fiber composites have stiffness and strength properties which are a function of time or have viscoelastic characteristics (23).

Because of these factors it is very important to perform the experiments under documented and similar conditions of humidity and temperature. It is recommended that all tests be performed as close to Standard Laboratory Atmosphere (SLA) conditions as possible. The SLA is air at 23 ± 2 °C and 50 ± 5% relative humidity.

DYNAMIC EXPERIMENTAL TECHNIQUES

Stiffness

As mentioned before, dynamic tests can be used to determine the dynamic modulus of elasticity, E', which is a measure of stiffness. In other words, we cannot determine the stiffness matrices under dynamic conditions. We can determine E_{11} and E_{22}, the modulus in the principal and orthogonal axis as well as material damping characteristics.

The forced vibration response technique is the most widely used method for characterizing the dynamic behavior of composites (24). Both stiffness and damping can be determined. The stiffness is found from the forced resonant frequency of a cantilever beam and damping from knowledge of the classical analytical relationships for flexural vibration of a beam.

Let us denote the dynamic modulus, sometimes referred to as the storage modulus, as E' which can be determined from the relationship (7):

$$\omega_r = \frac{(\lambda_r L)^2}{L^2} \left[\frac{E'I}{\mu}\right]^{1/2} \qquad [8]$$

where the eigenvalues, $\lambda_r L$, have been tabulated by Bishop and Johnson (25), μ is the mass per unit length, ω_r is the beam resonant circular frequency of mode r, I is the 2nd moment of area of the beam and L is the beam length.

The technique involves using a center-driven double-cantilever beam specimen. A sketch of this type of test specimen is shown in Figure 12.

Flexural vibrations of the one-piece specimen are induced by vertical motions of the shaker table which is mounted at the middle of the specimen. Vibration frequency and amplitude are controlled by adjusting the electrical current to the shaker coil. Specimen resonant frequency is determined by driving the beam at various resonant modes.

Strain gages would be mounted on the surface of the beam and an accelerometer mounted on the shaker. Resonant frequencies are then determined by varying the shaker frequency and observing the strain-acceleration Lissajous patterns on an oscilloscope as shown in Figure 13. This Lissajous pattern is produced by plotting the strain signal against the base acceleration signal. Beam resonant frequency is located by maximizing the ratio of strain amplitude to input acceleration amplitude.

The double-beam cantilever test specimen must be balanced to minimize frictional losses. By using the signals from strain gages mounted on both beams located equal distance from the base, the test apparatus can be balanced. The two strain gage signals from opposing beams are exactly in phase when the Lissajous pattern is 45-deg. line. Small weights can be attached to the end of the beams to balance the specimen. If the two beams are not in phase, the Lissajous pattern forms an ellipse. Having obtained the resonant frequency ω_r, the dynamic modulus E' is obtained by manipulating Equation 8. A reasonably sized test specimen would be 2.5-cm (1-in.) width and 30.5-cm (12-in.) double length (2-L).

Damping

Let us define an effective complex modulus, E*, with the relationship

$$E^* = E' + iE'' \qquad [9]$$

where E" is called the loss modulus (imaginary). The specimen loss factor, η_s, is related to the complex modulus by the equation (26)

$$\eta_s = \frac{E''}{E'} = 2\nu \qquad [10]$$

where ν is the damping ratio. Specimen damping can be computed by using the definition of specimen loss factor (26)

$$\eta_s = \frac{D_s}{2\pi U_s} \qquad [11]$$

where $$D_s = \pi V_o a_o \qquad [12]$$

and $$U_s = \frac{1}{2} \int_o^L \frac{M(x)^2}{E' I} \, dx \qquad [13]$$

where D_s and U_s are the energy dissapated per cycle and strain energy in the beam at maximum displacement respectfully. The unknown shear force, V_o, and bending moment, $M(x)$, are found from the characteristic function describing the mode shapes (25) and the measured strain at a known location on the beam. The base amplitude, a_o, can be found from the measured base acceleration and resonant frequency. Gibson (8) showed that the resulting equation for specimen loss factor is,

$$\eta_s = \frac{\lambda_r \phi'''(0) \phi_r'' (x_o) h \ddot{a}_o}{2 L \omega_r^2 \varepsilon(x_o)} \qquad [14]$$

The loss factor is always positive in this relationship because $\phi_r''(o)$ for a cantilever beam is negative (25). Equation 14 can be used to compute the loss factor from measured values of ω_r, $\ddot{a}_o$, $\varepsilon(x_o)$, h and L and tabulated values of λ_r, $\phi_r''(x_o)$, and $\phi_r'''(0)$ (25).

The testing technique described is referred to as the resonant-dwell technique (8) versus the bandwidth technique (5, 6). The forced vibration test was selected over the amplitude decay test not only because of the

ability to control both amplitude and frequency of vibration, but also because damping can be determined at a single frequency and amplitude. During resonant dwell testing, the specimen is usually driven in its first or 2nd mode; while the resonant frequency, input acceleration and bending strain are measured. Damping is determined using equation 14 and dynamic modulus (storage modulus) is determined using equation 8.

Tests should be performed at small amplitude-to-thickness ratios, w(L)/h, because of air damping. Gibson (8) performed tests as described using an aluminum specimen in air and in vacuum, and found that air damping is neglible when $w(L)/h < 0.5$.

To ascertain the effectivenss of frequency on stiffness and damping, the resonant-dwell technique can be used by driving the beam at higher modes. Using this technique, Schultz and Tsai (5) measured resonant frequencies as high as 10k Hz. These higher mode tests should be performed in a vacummn because of air frictional effects, i.e., air damping loss could become appreciable even at small amplitudes. Air damping would be proportional to velocity squared because of aerodynamic viscous drag effects.

Gibson (8) shows that thermoelastic loss factors are directly relatd to frequency, therefore, material heating could create problems. This investigator also reported excessive specimen loss factors at maximum strain amplitudes exceedings 10^{-3} for a [0°/90°] Scotchply specimen. Based upon this latter information, tests should be performed in the amplitude independent range, i.e., at $\varepsilon \leq 10^{-3}$.

PARTIAL RESULTS

A few tension tests have been performed on 8-ply T300/5208 (9) graphite-epoxy angle ply laminates. This laminate consisted of nomially 1-mm

(0.04-in.) thick material having a lay-up of $[0°, 45°, -45°, 90°]_s$. These tension tests were performed per ASTM standard test D3039-76 [11] as outlined in this report. The strain was measured along the principal (longitudinal) and orthogonal (transverse) axis; therefore, no shearing coupling data was determined, i.e., A_{16}.

The results of these tensile tests are shown in Table I, where orientation refers to the outer fiber alignment in the direction of applied tensile load. In other words, two types of tensile test samples were used, the first set was with the outer fibers aligned with the longitudinal specimen axis and the second set with the outer fibers orthogonal to the longitudinal axis.

Based upon a lamina thickness of 0.127-mm (0.005-in.) the laminate theory predicts $A'_{12} = A'_{21} = -5.756$ Gm/N for a total laminate thickness of 1.016-mm (0.040-in.). Inspection of Table I shows that $A'_{11} = A'_{22}$ within 1.2% and $A'_{12} = A'_{21}$ within 0.9%.

The main concern is to determine if the laminate theory is valid. Review of Table I shows that A'_{11} and A'_{22} were with in approximately 3%, also A'_{12} and A'_{21} were within approximately 4% when comparing laminate theory with experimental results. One could readily conclude that the laminate theory is accurate, at least for the limited extensional case considered.

Remembering that the laminate theory uses experiment results based on lamina experimental data, let us investigate lamina data for the T300/5208 composition. Lamina properties from various references are shown in Table II. Inspection of this table shows variation between the reported lamina

material characteristics of 35% for E_{11}, 7% for E_{22}, 30% for G_{12}, and 36% for ν_{12}. The comparison made in Table I was based upon O'Brien's (27) data because of the known similarity of composition and curing process.

One reasonable conclusion that can be made at this point in the experimental process is that the laminate theory is only as accurate as the lamina data. This conclusion is in turn only valid if we assume that the laminate experimental data being reported is composed of the lamina reported by O'Brien. In the future, it is highly recommended that lamina material characteristics E_{11}, E_{22}, G_{12} and ν_{12} be experimentally verified for each "batch" of laminate plates that is fabricated. This lamina data gathering should only be terminated when sufficient statistical information is collected which provides confidence in the repeatability of the lamina material fabrication process.

CONCLUSIONS AND RECOMMENDATIONS

1. Both dynamic and static material property measurements should be performed. Both laminate and single-ply tests are required. Variability of these properties will be dependent upon the actual materials used in fabricating the laminate (fibers and resin), the details of the manufacturing process, environmental conditions (temperature and moisture) and the actual test methods.
2. It is imperative that the laminate theory be verified under dynamic conditions. These studies should consider the frequency distribution of the excitation. This investigation should also involve short wave lengths and large amplitudes.

3. Very few standard test techniques are available for determining material properties of laminates. Many test techniques have been proposed but have not been accepted by the composite material testing community. The only standard test that is being used is for tensile testing of laminate specimens. There exist no tests for determining the dynamic stiffness matrix elements in extension, coupling or bending.
4. Short term goals include determining the dynamic stiffness and material damping characteristics of the laminates presently being investigated. The extensional and bending stiffness elements under static conditions should also be completed.

ACKNOWLEDGEMENTS

I thank Dr. Gene Goglia, Director of the NASA/ASEE Summer Faculty Fellowships Program, for giving me the opportunity to perform research at the NASA Langley Research Center. Great appreciation is extended to Dr. John S. Mixson for his guidance and support during the summer program. I also appreciated the help extended to me by Karen E. Heitman, Dr. C. Mei, C. Prasad, and Carl E. Rucker.

It should be noted that the study being reported is based upon a ten week period and was sponsored by the NASA/ASEE Summer Faculty Fellowship Program. The author had access to NASA Langley Research Center technical personnel as well as the Technical Library and reviewed approximately thirty reports.

REFERENCES

1. Mei, C. and Wentz, K. R., "Large-Amplitude Random Response of Angle-Ply Laminated Composites Plates," AIAA J., Vol. 20, No. 10, 1981, pp. 1450-1458.

2. Wentz, K. R., Paul, D. B., and Mei, C., "Large Deflection Random Response of Symmetric Laminated Composite Plates," Shock and Vibration Bullentin, Bulletin 52, Part 5, May 1982.

3. Mei, C., "Large Deflectin Multimode Response of Clamped Rectangular Panels to Acoustic Excitation," Vol. I, AFWAL-TR-83-3121, Dec. 1983.

4. Jones, R. M., "Mechanics of Composite Materials," McGraw Hill, 1975.

5. Schultz, A. B., and Tsai, S. W., "Dynamic Moduli and Damping Ratios in Fiber-Reinforced Composites," J. Composite Materials, Vol. 2, No. 3, July 1968, pp. 368-379.

6. Schultz, A. B., and Tsai, S. W., "Measurements of Complex Dynamic Moduli for Laminated Fiber-Reinforced Composites," J. Composite Materials, Vol. 3, July 1969, pp. 434-443.

7. Gibson, R. F., and Plunkett, R., "Dynamic Mechanical Behavior of Fiber-Reinforced Composites: Measurement and Analysis," J. Composite Materials, Vol. 10, Oct. 1976, pp. 325-341.

8. Gibson, R. F., and Plunkett, R., "A Forced Vibration Technique for Measurement of Material Damping," Experimental Mechanics, Vol. 17, No. 8, Aug. 1977, pp. 297-302.

9. DOD/NASA Advanced Composites Design Guide, July 1983.

10. Tsai, S. W., "Structural Behavior of Composite Materials," NASA CR-71, July 1964.

11. "Standard Test Method for Tensile Properties of Fiber-Resin Composites," ASTM Designation: D3039-76 (Reapproved 1982).

12. Spiegel, B. S., "An Experimental and Analytical Investigation of the Iosipescu Shear Test for Composite Materials," M.Sc. Thesis, Engr. Mech., Old Dominion University, Aug. 1984.

13. Herakovich, C. T., Bergner, H. W., and Bowles, D. E., "A Comparative Study of Composite Shear Specimen Using the Finite Element Method," ASTM STP 734, C. C. Chamis, Editor, ASTM PCN 04-734000-33, 1979, pp. 129-151.

14. Rouse, M., "Postbuckling of Flat Unstiffened Graphite-Epoxy Plates Loaded in Shear," AIAA Paper No. 85-0771-CP, 1985.

15. Iosipescu, N., "New Accurate Procedure for Single Shear Testing for Metals," J. Materials, Vol. 2, No. 3, Sept, 1967, pp. 537-566.

16. Slepetz, J. M., Zageski, T. F., and Novello, R., "In-Plane Shear Test for Composite Materials," AMMRC TR 78-30, July 1978.

17. Snell, M. B., and Marchant, M. J., "Determination of the Flexural Stiffness of Carbon Composite Plates by Holographic Interferometry," J. Strain Analysis, Vol. 19, No. 4, 1984 pp. 249-259.

18. Marchant, M. J., and Snell, M. J., "Determination of the Flexural Stiffness of Thin Plates from Small Deflection Measurements Using Optical Holography," J. Strain Analysis, Vol. 17, No. 1, 1982, pp. 53-61.

19. Colles, M. J. and Swift, D. W., "Measurement of Curvature and Bending Stiffness of Thin Carbon Composite Plates Using Holographic Interferometry," SPIE (The International Society for Optical Engineering), Vol. 369 Max Born, 1982, pp. 502-509.

20. Hernessey, J. M., Whitney, J. M., and Riley, M. B., "Experimental Methods of Determining Shear Modulus of Fiber Reinforced Composite Material," AFML-TR-65-42, Sept. 1965.

21. Maymon, G., Briley, R. P., and Rehfield, L. W., "Influence of Moisture Absorption/Elevated Temperature of the Dynamic Behavior of Resin Matrix Composites: Preliminary Results," Advanced Composite Materials-Environmental Effects, ASTM STP 658, 1978.

22. Whitney, J. M., and Husman, G. E., "Use of the Flexure Test for Determining Environmental Behavior of Fibrous Composites," Exptl. Mech. Vol. 18, No. 5, May 1978, pp. 185-190.

23. Hiel, C., Cardon, A. H., and Brinson, H. F., "The Nonlinear Viscoelastic Response of Resin Matrix Composite Laminates," NASA CR 3772, July 1984.

24. Bert, C. W., and Clary, R. R., "Evaluation of Experimental Methods of Determining Dynamic Stiffness and Damping of Composite Materials," Composite Materials: Testing and Design (Third Conference) ASTM STP 546, 1974, pp. 250-265.

25. Bishop, R. E. D., and Johnson, D. C., "The Mechanics of Vibration," Cambridge University Press, 1960, p. 382.

26. Lazan, B. J., "Damping of Materials and Members in Structural Mechanics," Pergamon Press, Oxford, 1968.

27. O'Brien, T. K., "Mixed-Mode Strain-Energy-Release Rate Effects on Edge Delamination of Composites," ASTM STP 836, pp. 125-142.

28. Soni, S. R., "A New Look at Commonly Used Failure Theories in Composite Laminates," AIAA CP 831, 24th Structures, Structural Dynamics and Materials Conference, May 2-4, 1983, Part I, pp. 171-179.

29. Ryder, J. T., S Crossman, F. W., "A Study of Stiffness, Residual Strength and Fatigue Life Relationships for Composite Laminates," NASA CR-172211, October, 1983.

TABLE I

T300/5208 Laminate

8-Ply Experimental Extensional Stiffness Data

Sample Comment	Orien. (deg)	t (mm)	A'_{11} ($G\frac{m}{N}$)	A'_{22} ($G\frac{m}{N}$)	$-A'_{12}$ ($G\frac{m}{N}$)	$-A'_{21}$ ($G\frac{m}{N}$)	E_{11} (GPa)	E_{22} (GPa)	V_{12} (unitless)
A-1-T	0	1.054	17.96	---	5.389	---	52.18	---	0.300
A-2-T	0	1.062	18.34	---	5.629	---	51.37	---	0.304
A-3-T	0	1.044	18.43	---	5.455	---	51.99	---	0.298
A-4-T	0	1.034	18.63	---	5.507	---	51.93	---	0.296
A-5-T	0	1.064	18.03	---	5.282	---	52.13	---	0.304
A-6-T	0	1.186	18.49	---	5.575	---	45.63	---	0.305
A-7-T	0	1.036	18.62	---	5.656	---	51.82	---	0.304
B-1-T	90	1.034	---	18.36	---	5.511	---	52.70	0.300
B-2-T	90	1.029	---	18.45	---	5.647	---	52.70	0.306
B-3-T	90	1.039	---	18.79	---	5.356	---	51.24	0.293
B-4-T	90	1.034	---	17.93	---	5.511	---	53.96	0.307
B-5-T	90	1.041	---	17.39	---	5.611	---	52.22	0.323
B-6-T	90	1.034	---	18.00	---	5.670	---	53.73	0.315
mean	---	1.053	18.36	18.15	5.499	5.551	51.01	52.76	0.304
6*	---	0.041	0.27	0.49	0.134	0.117	2.39	1.00	0.008
% Diff.	---	3.7	2.7	3.7	4.5	3.6	8.7	5.6	2.0

Theoretical Values: $A'_{11} = A'_{22} = 18.86$ Gm/n, $A'_{12} = A'_{21} = 05.756$ Gm/n and $t = 1.016$ mm,
DOD/NASA design data: $E_{11} = E_{22} = 55.9$ GPa and $V = 0.31$

* Standard deviation

TABLE II

T300/5208 Lamina Properties

E_{11} (GPa)	E_{22} (GPa)	G_{12} (GPa)	ν_{12} ---	Reference
147	10.9	6.41	0.38	(9)
134	10.5	5.5	0.30	(27)
181	10.3	7.17	0.28	(28)
163	10.2	6.48	0.39	(29)

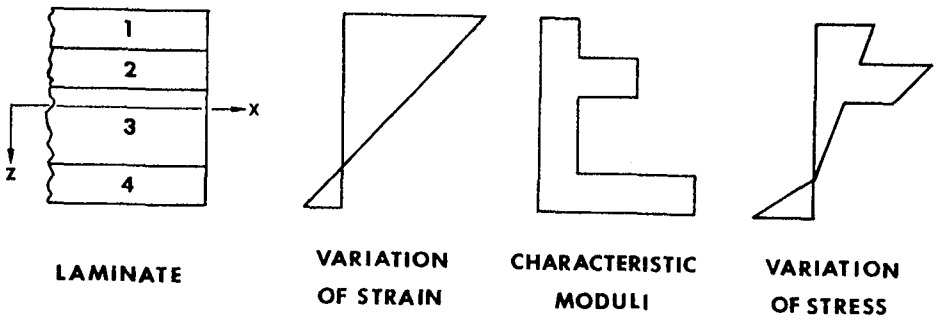

Figure 1. Hypothetical variation of strain and stress through the laminate thickness. (4)

Type of Reinforcement	Continuous Fibers		Discontinuous Fibers	
	mm	in.	mm	in.
Boron	0.508 to 2.54	0.020 to 0.100	1.016 to 5.08	0.040 to 0.200
Graphite	0.508 to 2.54	0.020 to 0.100	1.016 to 5.08	0.040 to 0.200
Glass	0.762 to 3.275	0.030 to 0.125	1.524 to 6.55	0.060 to 0.250

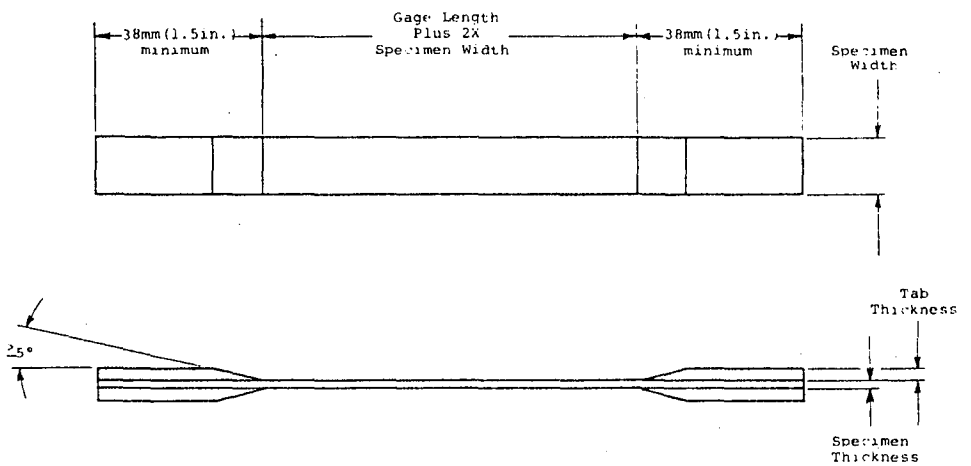

NOTE—Bond laminate tabs on two sides and at both ends. Tabs are applied to the end of the test composite with a suitable adhesive. Each tab is a minimum of 38 mm (1.5 in.) long by the width of the laminate and a thickness of approximately 1.5 to 4 times the thickness of the test composite.

Figure 2. Tensile Test Specimen (11)

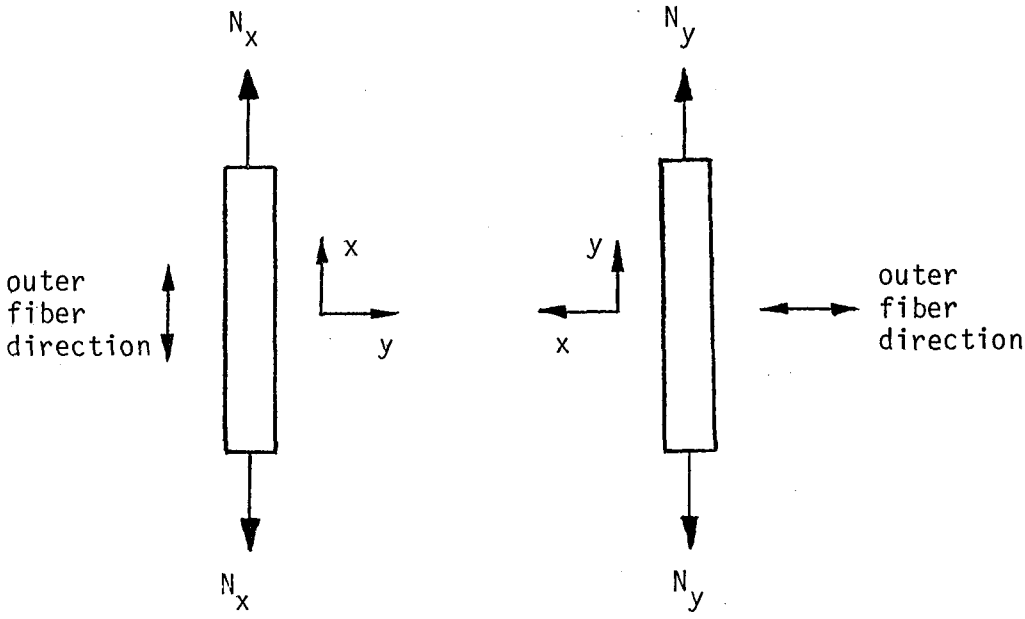

Figure 3.- Tensile specimen test arrangement.

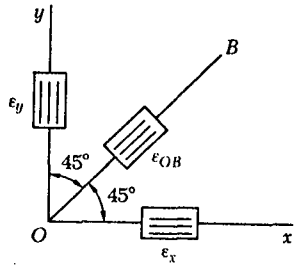

Figure 4.- Strain gage rosette.

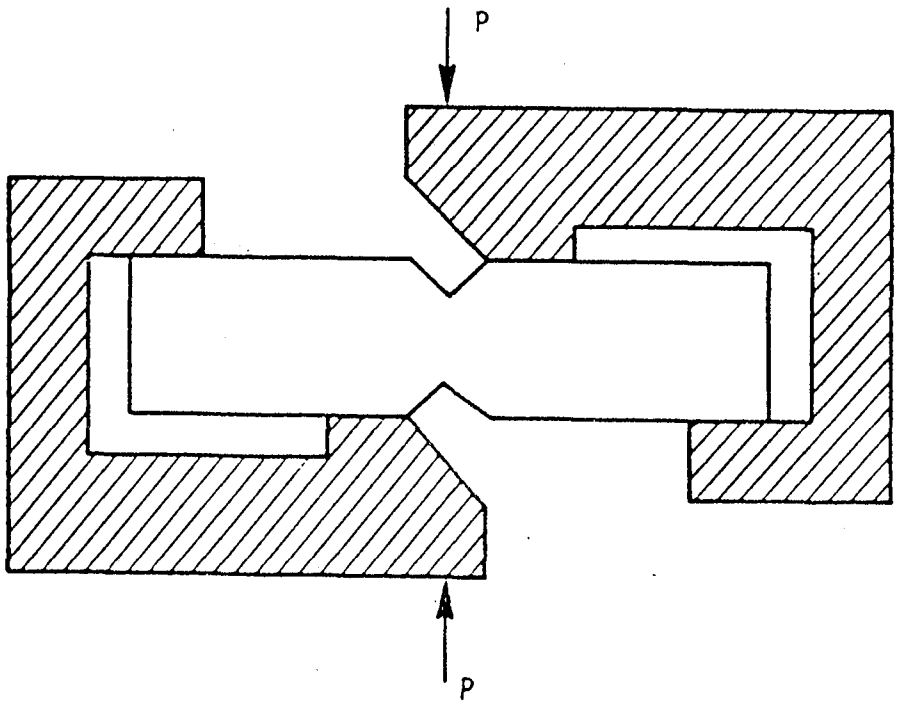

Figure 5.- Schematic of the Iospiescu shear test fixture (12).

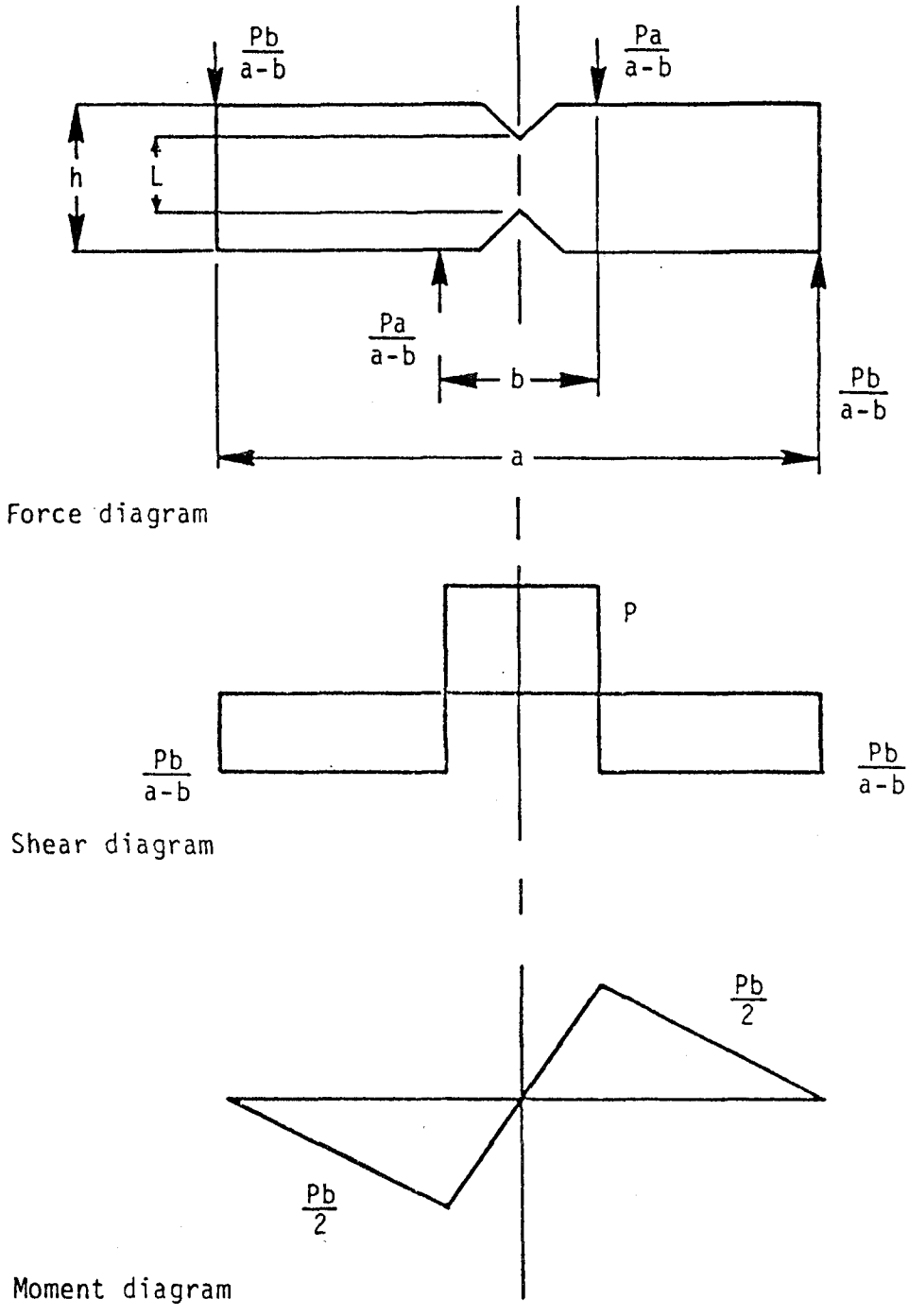

Figure 6.- Force, shear and moment diagrams of the Iosipescu shear test (12).

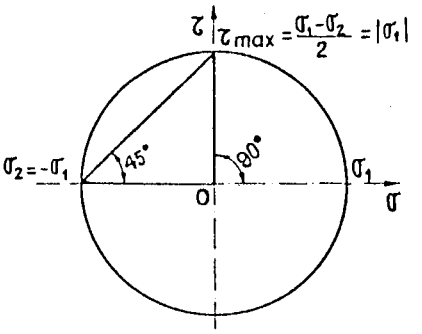

Figure 7.- Mohr's circle for bidimensional pure shear stress state (15).

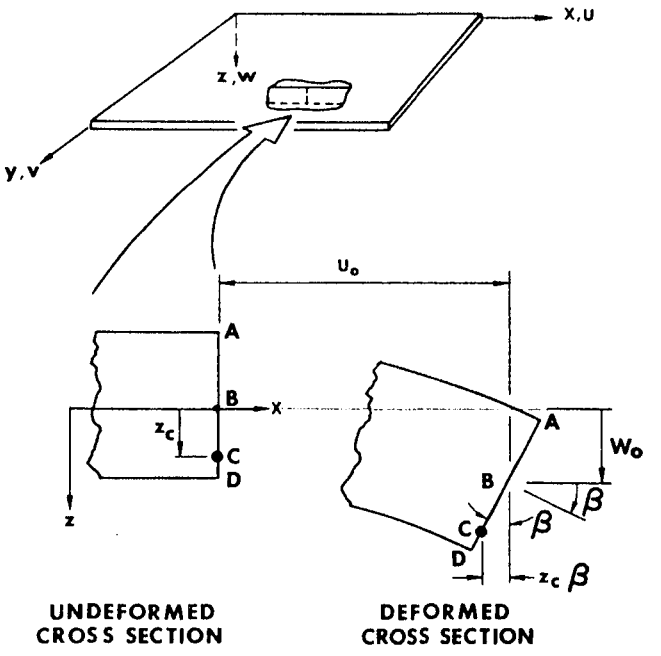

Figure 8.- Geometry of deformation in the x-z plane (4).

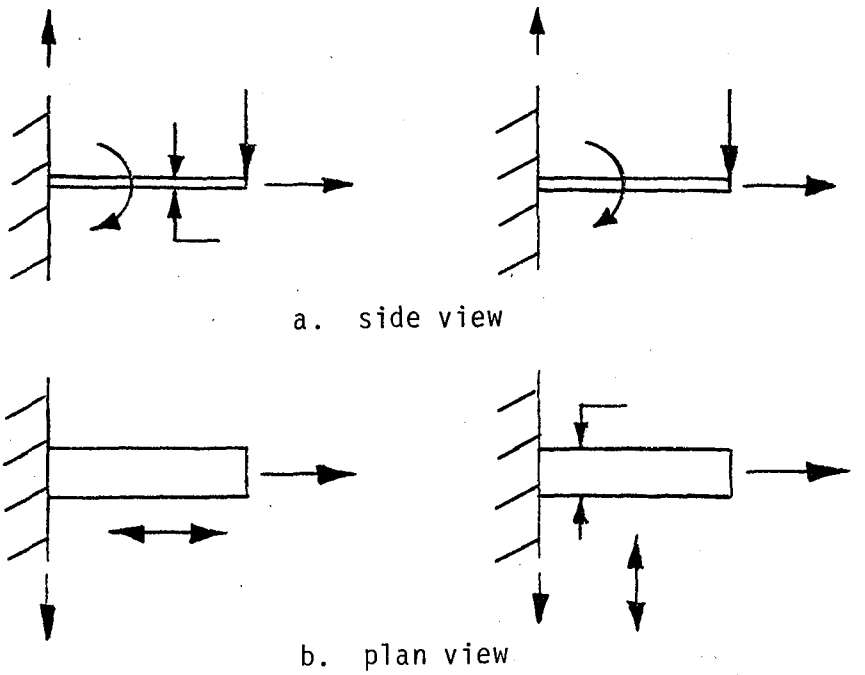

a. side view

b. plan view

Figure 9.- Simply loaded cantilever beam.

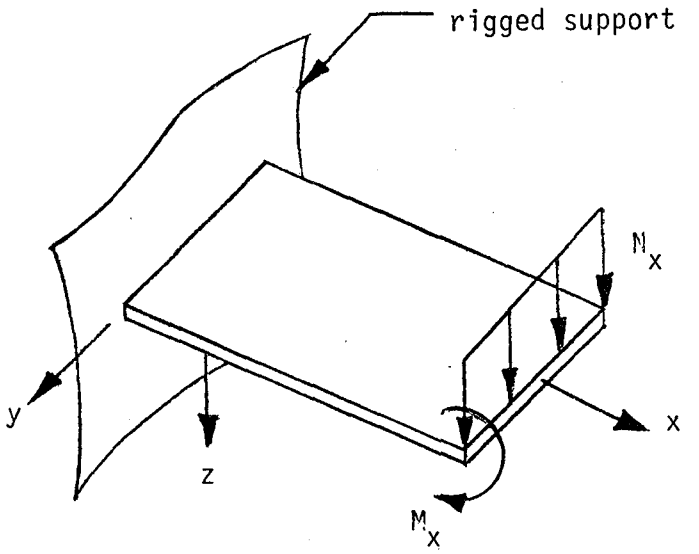

Figure 10.- Cantilever beam.

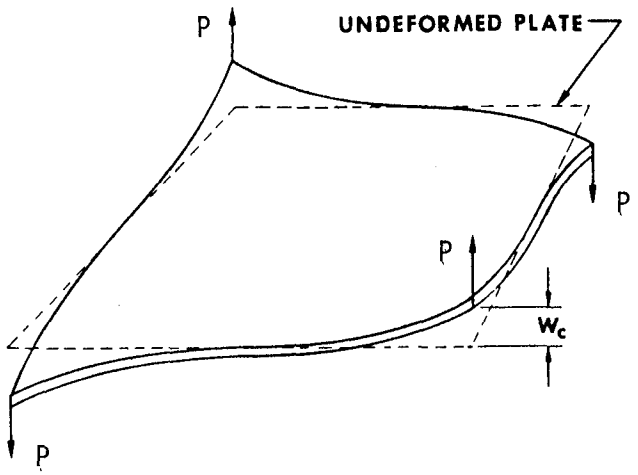

Figure 11.- Twisting of a square plate (4).

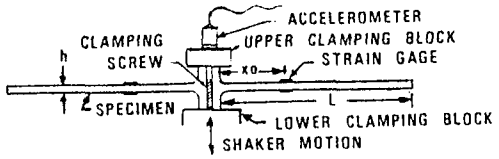

Figure 12.- Double-cantilever beam specimen configuration (8).

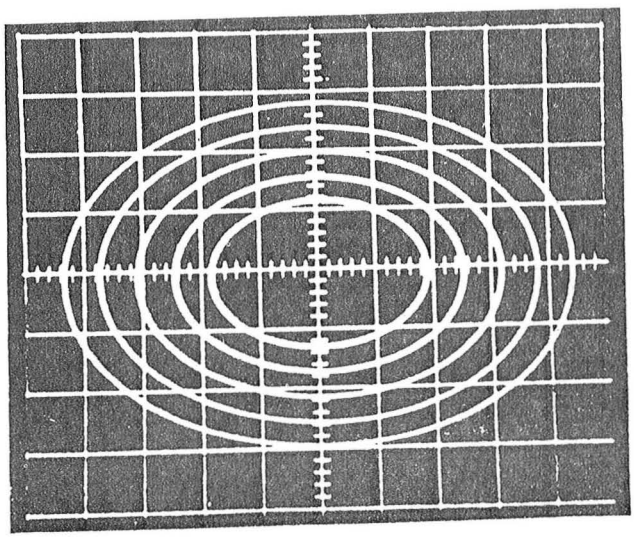

Figure 13.- Lissajous patterns generated by strain (vertical) and acceleration (horizontal) signals (8).

1. Report No.	2. Government Accession No.	3. Recipient's Catalog No.
NASA TM-87601		

4. Title and Subtitle	5. Report Date
INVESTIGATION OF COMPOSITE MATERIALS PROPERTY REQUIREMENTS FOR SONIC FATIGUE RESEARCH	August 1985
	6. Performing Organization Code: 505-33-53-03
7. Author(s): Howard V. L. Patrick*	8. Performing Organization Report No.
	10. Work Unit No.
9. Performing Organization Name and Address: NASA Langley Research Center, Hampton, VA 23665-5225	11. Contract or Grant No.
	13. Type of Report and Period Covered: Technical Memorandum
12. Sponsoring Agency Name and Address: National Aeronautics and Space Administration, Washington, DC 20546	14. Sponsoring Agency Code

15. Supplementary Notes *Embry-Riddle Aeronautical University, Daytona Beach, Florida

The author performed this work while working at Langley under the 1985 NASA/ASEE Summer Faculty Fellowship Program.

16. Abstract

This paper presents experimental techniques for determining the extensional and bending stiffness characteristics for symmetric laminates. Vibrational test techniques for determining the dynamic modulus and material damping are also discussed.

Partial extensional stiffness results intially indicate that the laminate theory used for predicting stiffness is accurate. It is clearly shown that the laminate theory can only be as accurate as the physical characteristics describing the lamina, which may vary significantly.

It is recommended that all of the stiffness characteristics in both extension and bending be experimentally determined to fully verify the laminate theory. Dynamic modulus should be experimentally evaluated to determine if static data adequately predicts dynamic behavior. Material damping should also be ascertained because laminate damping is an order of magnitude greater than found in common metals and can significantly effect the displacement response of composite panels.

17. Key Words (Suggested by Author(s))	18. Distribution Statement
Sonic fatigue Material properties Composites	Unclassified - Unlimited Subject Category - 71

19. Security Classif. (of this report)	20. Security Classif. (of this page)	21. No. of Pages	22. Price
Unclassified	Unclassified	36	A03

For sale by the National Technical Information Service, Springfield, Virginia 22161